Available online at www.sciencedirect.com

ScienceDirect

Procedia Structural Integrity 12 (2018) 578–588

Structural Integrity Procedia

www.elsevier.com/locate/procedia

AIAS 2018 International Conference on Stress Analysis

A sensitivity analysis on the damage detection capability of a Lamb waves based SHM system for a composite winglet

A. De Luca[a]*, D. Perfetto[a], A. De Fenza[b,c], G. Petrone[b], F. Caputo[a]

[a]*Department of Engineering, University of Campania "L. Vanvitelli", Via Roma 29, 81031 Aversa, Italy*
[b]*Department of Industrial Engineering – Aerospace Division, Università degli Studi di Napoli "Federico II", Via Claudio 21, 80125, Napoli, Italy*
[c]*Department of Bioengineering and Aerospace Engineering, Universidad Carlos III de Madrid, Av. de la Universidad 30, 28911 Leganés, Spain*

Abstract

Lamb waves based Structural Health Monitoring (SHM) systems, thanks to their high sensitivity to damage detection and the ability to travel over a long distance with low power consumption, are founding increasing industrial applications, especially in the aerospace field, where airworthiness authorities require that composite materials in primary structures must remain undamaged during the in-service life. In order to tolerate damage and monitor its severity and, consequently, to repair the structure only when strictly needed, the use of SHM systems appears to be an efficient solution providing benefits for the current design practice. The continuous assessment of the structural integrity, which can be accomplished by SHM systems, can play a key-role to achieve a less-conservative design as well as to facilitate maintenance operations.
This paper deals with a sensitivity analysis, based on the Finite Element (FE) theory, aimed to investigate numerically the influence of the damage orientation on the damage detection capability of a Lamb waves based SHM system arranged on a damaged Glass Fiber Reinforced Polymer composite winglet. Damage detection sensitivity has been measured by analyzing the interaction between the modelled damages and guided waves under a specific central frequency. Signals recorded at different locations by piezoelectric sensors have been compared with the baseline signals achieved under a pristine configuration of the winglet by means of a damage index. A specific trend of the considered damage index has been found out as function of the damage orientation.

* Corresponding author. Tel.: +39 081 5010 318
E-mail address: alessandro.deluca@unicampania.it

2452-3216
10.1016/j.prostr.2018.11.061

Keywords: Guided Lamb waves; FE modelling; Damage index; Structural Health Monitoring; Sensitivity analysis

1. Introduction

Structural Health Monitoring (SHM) systems can significantly improve the aerospace design current practice in terms of sizing and manufacturing costs (Caputo et al. (2018), Worden et al. (2004), Reda et Lucero (2005), Chiu et al. (2009)), especially when primary components are made of composite materials.

The use of composite materials, in fact, is still limited due to their susceptibility to manufacturing defects and in-service damages that can lower substantially their residual strength (Sepe et al. (2016), Riccio et al. (2017) - Composites Part B, Riccio et al. (2016), Riccio et al. (2017) - Engineering Failure Analysis). Actually, it is not yet possible to take completely advantage by the high specific strength characterizing such materials due to the application of the large safety factors that currently are applied during the design phase to allow the structure to sustain the ultimate load also when affected by damages (Mircea et Holger (2010), De Luca et al. (2018) - Composites Part B: Engineering).

Specifically, Barely Visible Damages (BVDs) (Russo et al. (2017), Lopresto et al. (2013), Liv et al. (2017)) can play a critical role, since they can lead the structure to a catastrophic failure, because of the not easy detectability. Under this scenario, the continuous monitoring offered by the SHM systems can give an important contribution in the current design practice (De Luca et al. (2018) - Procedia Structural Integrity). The possibility to detect in real time the damages onset can provide a consequent lowering of the safety factors: a detectable damage can be, in fact, easily repaired. Moreover, SHM systems provide benefits also in terms of manufacturing costs. According to the Damage Tolerance philosophy, several inspections, aimed to the damage detection, must be carried out during the real life of the components. Such inspections, which are often expensive, time-consuming and require skilled workers, can be replaced actually by the application of SHM systems.

Nowadays, among the several SHM systems types, a special attention is being dedicated to ultrasonic guided-waves, such as Lamb waves (Lamb (1917), Ciminello et al. (2017), Su et Ye (2009), Lee et al. (2003), De Luca et al. (2016), Sharif-Khodaei et Aliabadi (2014)). This technology is based on the fact that the propagation mechanisms of the guided waves depend strictly on the medium where they propagate through. As a consequence, by activating the guided waves in a thin-walled structure by means of one or more actuators, they will start to propagate in correspondence of its free surfaces. The modes induced by the guided waves can be recorded by means of receiving sensors arranged at different locations of the structure. Since wave modes can be altered by the presence of a damage (De Fenza et al. (2015), Sorrentino et De Fenza (2017) – 11th International Workshop on Structural Health Monitoring, Sorrentino et De Fenza (2017) - Journal of Mechanical Engineering Science, De Fenza et al. (2017), Sorrentino et al. (2018)), by comparing the signals recorded in a damaged configuration with the signals recorded in a reference configuration (pristine one), it is possible to estimate the damage severity.

Lamb waves are founding increasing applications thanks to their sensitivity to the damage detection, extent of the monitored area and low costs (Su et Ye (2009)). Nevertheless, their application can become difficult and tricky, especially when it is aimed to monitor the structural integrity of composite structures (Su et Ye (2009)). Damage detection sensitivity provided by Lamb waves depends basically on the SHM system setup as well as on the sensors locations. However, the setup phase of guided waves in composites is not as trivial as for conventional materials (Frederick (1962), Worlont (1961) and Rose (2001)). For these reasons, numerical simulations can be very helpful to support the set up phase of real applications and to better understand physics of guided waves (De Luca et al. (2018) - Composites Part B: Engineering, De Luca et Al (2016) and Sharif-Khodaei et Aliabadi (2014)). Among the several numerical methods, Finite Element (FE) one appears to be the most appropriate technique; in the last decades, the most of the commercial FE codes, in fact, has been significantly improved in modelling multi-layered composites, material inhomogeneity and anisotropy that can lead the onset of new propagation mechanisms respect to isotropic materials that cannot be neglected. It is not negligible also the dependence of wave modes on laminate layup configurations, fibers direction, frequency and interface conditions.

In this paper, Lamb wave propagation in a damaged blended double-curvature GFRP (Glass Fiber Reinforced Polymers) winglet has been numerically simulated. Specifically, the research activity proposed herein is an evolution of the research line carried out by the authors on guided waves based SHM systems applied to complex composite

structures. The investigated test article, consisting in the aforementioned winglet, has been previously investigated experimentally and numerically under damaged and pristine configurations and some of the results are presented in De Luca et al. (2018) - Key Engineering Materials.

The experimental tests, carried out on the test article, have been presented in De Fenza et al. (2017). Specifically, Lamb waves were activated in the winglet, through different actuation signals, under both pristine and damaged configurations. Damages were introduced by means of a Low Velocity Impact (LVI) test, with an energy level of 12.5 J and a drop mass of 0.8 kg, performed in the area surrounded by sensors 4, 5, 7 and 8, highlighted in red in Fig. 1. Damages were detected by means of C-SCAN method, providing precise information about the damage in terms of in-plane extension (equal to ~ 160 mm^2) at a laminate thickness depth of 1.61 mm, starting from the impacted surface. Concerning the numerical activities, in De Luca et al. (2018) - Key Engineering Materials, two FE models for the simulation of the guided waves propagation in both damaged and pristine configurations were presented. The experimental results achieved in De Fenza et al. (2017) were used in De Luca et al. (2018) - Key Engineering Materials to assess the reliability of the proposed FE models. By comparing the experimental and numerical results, it was found out that both FE models were able to provide good levels of accuracy. Moreover, it was found out that shell elements are able to simulate accurately the guided wave propagation mechanisms also in complex (strong curvatures) composite structures as well as to reduce the computing time of about 90 % respect to 3D finite elements. Concerning the damaged configuration of the winglet, different techniques were investigated in De Luca et al. (2018) - Key Engineering Materials to reproduce numerically LVI damages in terms of extension.

In this paper, a step forward the study of the damage orientation influence on the damage detection capability of the considered SHM system has been proposed. According to the literature, several studies have been carried on such topic (i.e. De Luca et al. (2018) - Procedia Structural Integrity), but no works involving complex structures have been presented yet. This research activity has been performed only through numerical simulations. However, as a result of the good level of accuracy showed by the FE models presented by the authors in De Luca et al. (2018) - Key Engineering Materials, by a Certification by Analysis (CBA) point of view, the reliability of the numerical results here provided can be consequently considered demonstrated.

Nomenclature

SHM	Structural Health Monitoring
BVD	Barely Visible Damage
FE	Finite Element
GFRP	Glass Fibre Reinforced Polymers
LVI	Low Velocity Impact
NPW	Nodes per Wavelength
CBA	Certification by Analysis
A	displacement amplitude coupled to the actuation signal in Volt
t	wave propagating duration
f_c	central frequency of the excitation signal
V	maximum applied voltage
n	number of cycles within the window
D_{IRMSD}	Root Mean Square Deviation Damage Index
P_k	baseline signal
D_k	signal captured under damaged configuration of the structure
K	the generic sampling point of the discretized Lamb wave signal
N	total of sampling points
PZT	Piezoelectric
ACT	Actuator
DI	Damage Index
S_0	Symmetric 0 waves mode

2. Test Article

The test article described in this paper has been widely described in De Fenza et al. (2017). Basically, it consists of a blended winglet for a small aircraft (Fig. 1.a), made of GFRP laminates and foam layers in the inner parts (green and yellow zones in Fig. 1.b) and GFRP laminates in the outer ones (red and blue zones in Fig. 1.b). The spar (showed in azure in Fig. 1.b) is made of a high performance low density foam core. The mechanical properties of the lamina are listed in Table 1 (De Fenza et al. (2017)).

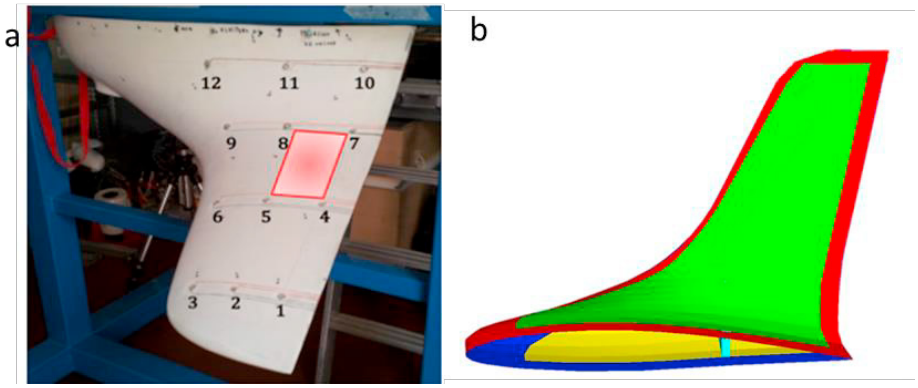

Fig. 1. (a) test article; (b) test article draft.

Table 1. Lamina material properties.

Material properties	Foam	Fiberglass
Young modulus [GPa]	1.3	-
Longitudinal Young modulus [GPa]	-	14
Transversal Young modulus [GPa]	-	8.0
Shear modulus [GPa]	0.303	-
Shear modulus [GPa]	-	4.0
Poisson's ratio	0.32	0.05
Mass density [kg/m^3]	112	1550

The winglet has been equipped with 12 piezoelectric (PZT) sensors (11 acting as receiver and 1 as actuator (ACT)), as shown in Fig. 1.a. LVI damages were introduced in the area surrounded by sensors 4, 5, 7 and 8, highlighted in red in Fig. 1. As aforementioned, damages were detected by means of C-SCAN method, providing precise information about the damage in terms of in-plane extension (equal to ~ 160 mm^2) at a laminate thickness depth of 1.61 mm, starting from the impacted surface.

Winglet skin is characterized by stacking sequences different for zone to zone, as shown in Table 2. Colors recalled in Table 2 are associated to the skin areas shown in Fig. 1.b.

Table 2. Stacking sequence for the different winglet skin regions.

External Upper (red)			Internal Upper (green)			External Lower (blue)			Internal Lower (yellow)		
Ply	θ	Material	Ply	θ	Material	Ply	θ	Material	Ply	θ	Material
1	0°	Fiberglass	1	0°	Fiberglass	1	0°	Fiberglass	1	0°	Fiberglass
2	±45°	Fiberglass	2		Foam	2	±45°	Fiberglass	2		Foam
3	±45°	Fiberglass	3	±45°	Fiberglass	3	±45°	Fiberglass	3	±45°	Fiberglass
4	±45°	Fiberglass	4	±45°	Fiberglass	4	±45°	Fiberglass	4	±45°	Fiberglass

5	0°	Fiberglass	5	±45°	Fiberglass		5	0°	Fiberglass
			6	0°	Fiberglass				

3. FE model

Starting from the FE model presented by De Luca et al. (2018) - Key Engineering Materials, the numerical investigation presented herein has been performed by introducing in the FE two damage types (in two separate analyses) different by each other only for the orientation. The two damage orientations are shown in Fig. 2.

Damages have been modelled according to the softening and deleting techniques discussed by authors in De Luca et al. (2018) - Key Engineering Materials. The former consists in modelling the damage by degrading the elastic material properties of 70%, whilst the latter in introducing a notch by deleting the elements. The degradation factor of 70% has been chosen in order to simulate a damage as severe as the one modelled according to the deleting technique. The application of a greater factor can lead to numerical issues. Other authors (i.e. Sharif-Khodaei et Aliabadi (2014)) considered a degradation factor of 50%.

Other damages modelling techniques can be considered. For example, De Luca et al. (2018) – Composite Part B modelled LVI damages by simulating the related impact event. However, this technique can be high time-consuming, especially for complex structures as the investigated winglet.

Damages have been modeled in the area highlighted in Fig. 2.

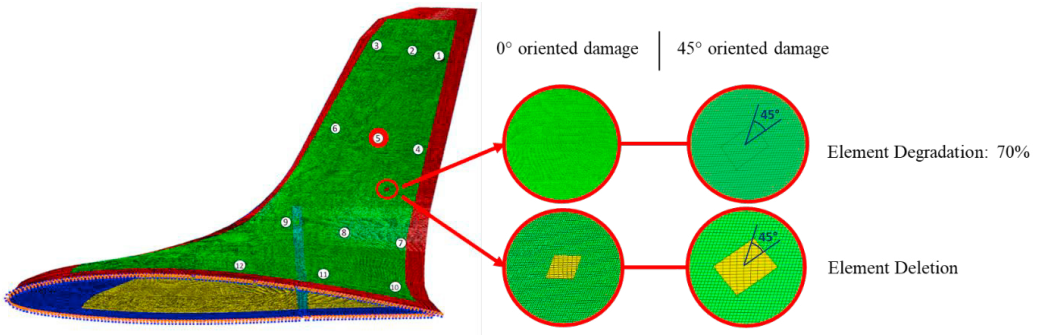

Fig. 2. Modelled damages in the winglet.

The winglet for both pristine and damaged configurations has been modelled by choosing an average characteristic length of the finite elements equals to 0.5 mm, corresponding to about 30 NPW with a central frequency of 100 kHz. A 4.5-cycle sine-burst actuation signal, with a central frequency of 100 kHz has been considered for all analyses. As a result, the skin has been modelled with 791111 shell elements and 792691 nodes (characteristic length of 0.5 mm), the sensors with 16005 three-dimensional brick elements and 22880 nodes (characteristic length of 0.25 mm) and the spar with 326040 brick elements and 347944 nodes (characteristic length of 0.5 mm). Actuator has been located in position 5, as shown in Fig. 2.

Concerning the modelling of the actuation signal, the same technique presented by De Luca et al. (2018) - Key Engineering Materials has been used. Radial displacements along the upper circumference of the actuator, equivalent to the actuation signal in voltage, have been applied (Su et Ye (2009)). The equivalent displacements can be achieved by means of Equation 1 (Su et Ye (2009)):

$$A(t)=\frac{1}{2}V\left[1-\cos\left(\frac{2\pi tf_c}{n}\right)\right]\sin\left(2\pi tf_c\right) \tag{1}$$

where, A is the amplitude, t is the wave propagating duration, f_c is the central frequency of the excitation signal, V is the maximum applied voltage and n is the number of cycles within the signal window (n=4.5).

All analyses have been performed within an explicit environment since the wave propagation is a dynamic problem. The numerical modelling has been performed by using Abaqus® ver. 6.14 finite element code.

In order to investigate the effects of the damage orientation on the wave propagation in a such complex structure, the signals recorded by the sensors arranged on the damaged winglet have been compared, through a damage index (DI), with the baseline ones acquired in the pristine configuration. The Root Mean Square Deviation (RMSD) Damage Index, D_{IRMSD} (Su et Ye (2009)), given by Equation 2, has been used.

$$DI_{RMSD} = \sqrt{\frac{\sum_{k=1}^{N}(D_k - P_k)^2}{\sum_{k=1}^{N}(P_k)^2}} \tag{2}$$

The DI_{RMSD} compares the pristine signal, P_k, captured in the initial state of the structure (undamaged), and the signal captured under another state of the structure, such as after impact damage occurs, D_k. k is the generic sampling point of the discretized Lamb wave signal and N is the total of sampling points.

By a numerical point of view, the predicted recorded signals are calculated as the average of the in-plane strains read by all nodes defining each sensor (Su et Ye (2009)).

4. Results and discussion

The post-processing of the numerical results, in terms of recorded signals, has been made through an own Matlab® routine. As aforementioned the two damage types have been modeled according to the softening and deleting techniques. The signals predicted under the two damage configurations have been compared to each other. Fig. 3 compares the signals achieved by modelling both 45° and 0° oriented damages according to the deleting technique. Whilst, Fig. 4 compares the signals achieved by modelling both 45° and 0° oriented damages according to the softening technique.

Each signal has been post-processed by normalizing it respect to the absolute maximum among all signals. The maximum value has been achieved in correspondence of sensor 6.

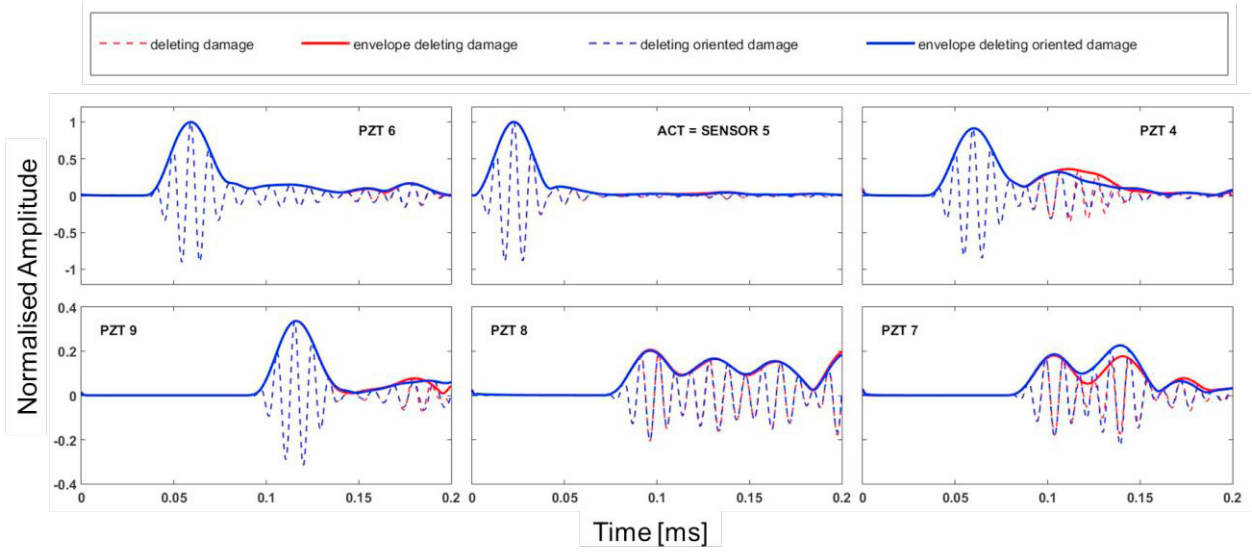

Fig. 3. Numerical signals referred to both 45° and 0° oriented damages, modelled according to the deleting technique.

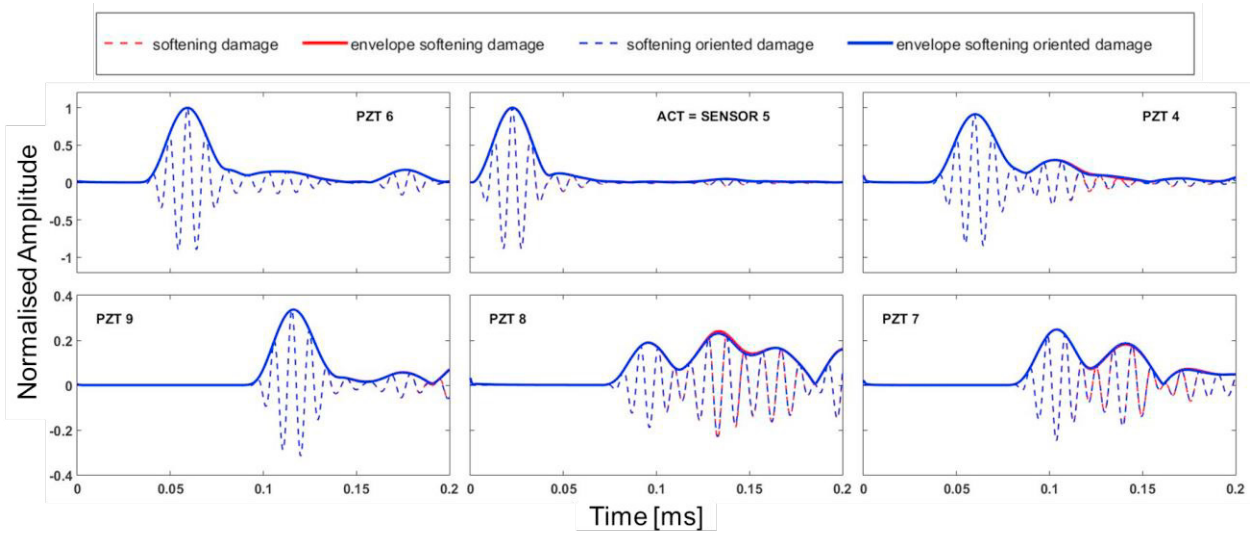

Fig. 4. Numerical signals referred to both 45° and 0° oriented damages, modelled according to the softening technique.

In order to improve the results readability, only signals recorded at sensors 4, 6, 7, 8 and 9 (sensors closest to the damage) have been reported in Fig. 3 and 4. Specifically, according to these figures, it can be noticed that, the damage orientation produces clear effects when the damage is modelled according to the deleting technique.

Fig. 5 shows the global displacements involving the winglet area affected by the damage due to the wave propagation, at selected instants of time. Specifically, figures denoted with letter (a) represent the winglet configuration, at same selected frames, where the 45° oriented damage is modelled according to the deleting technique; figures denoted with letter (b) represent the winglet configuration where the 45° oriented damage is modelled according to the softening technique; figures denoted with letter (c) represent the winglet configuration where the 0° oriented damage is modelled according to the deleting technique; figures denoted with letter (d) represent the winglet configuration where the 0° oriented damage is modelled according to the softening technique.

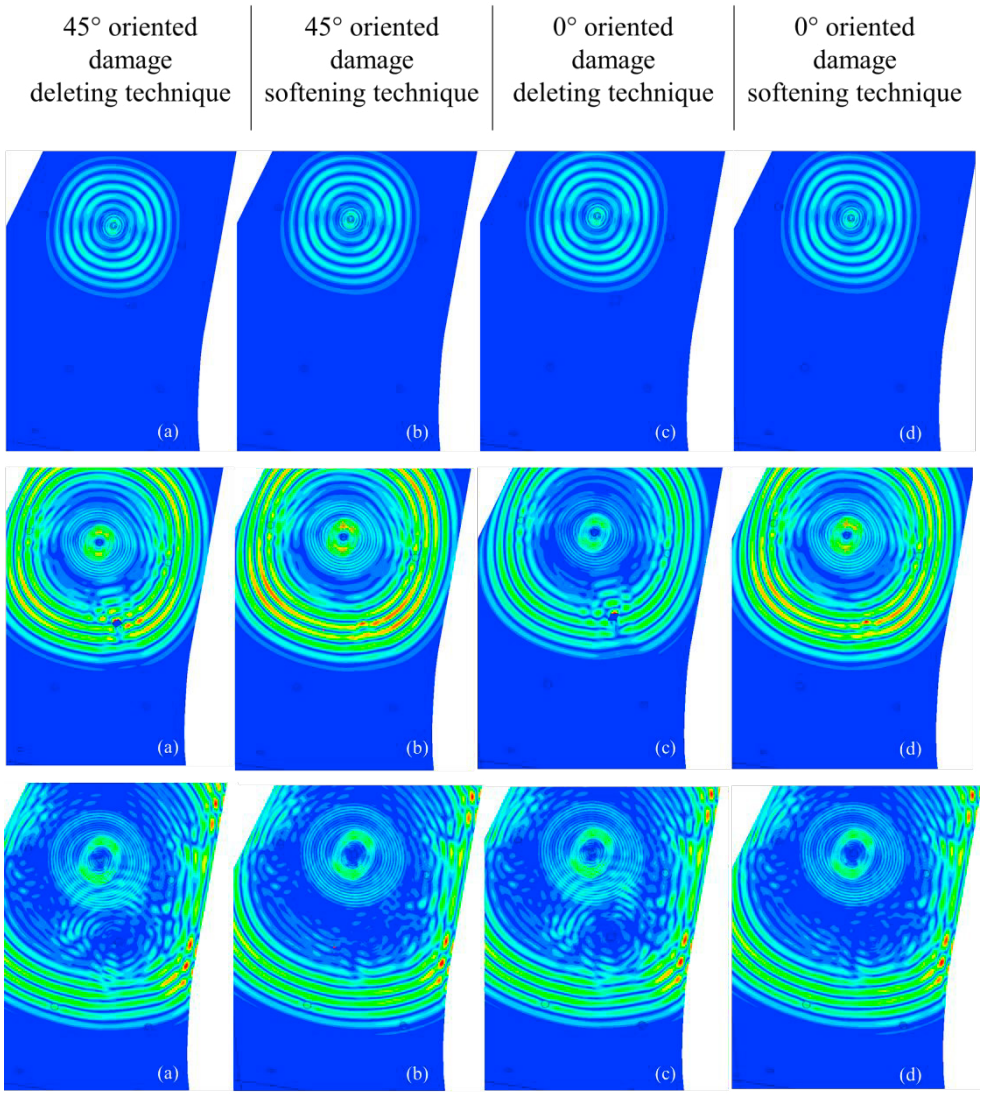

Fig. 5. Displacement field induced by the wave propagation at different frames.

According to Fig. 5, it can be noticed that damages modeled according to the deleting technique (Fig. 5.b and Fig. 5.d) reflect guided waves much more than damages modeled according to the softening technique. This can be attributed to the fact that the deleting technique introduces new free edges inside the winglet and to the fact that the softening technique introduces a less severe damage, since the elastic material properties are lowered of 70%.

Fig. 6 shows the comparison of the RMSD damage index values, achieved by the experimental tests and by all performed simulations. Only the damage indexes calculated with reference to the sensors surrounding the damage (sensors 4, 6, 7, 8 and 9) have been reported in Fig. 6.

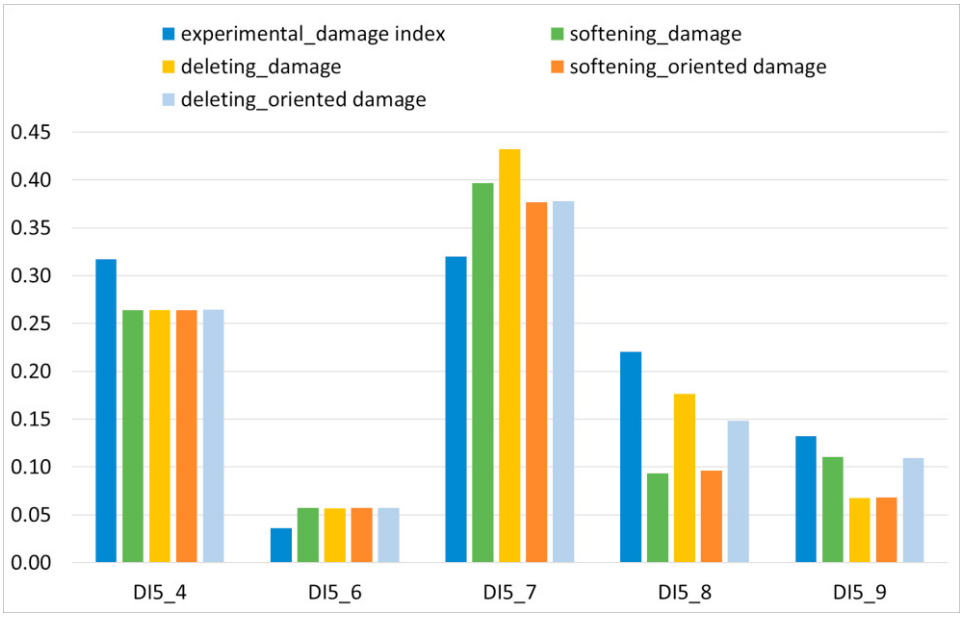

Fig. 6. Damage indexes comparison.

Damage indexes shown in Fig. 6 have been calculated by comparing only the first waves package of the pristine and "damaged" recorded signals. This choice depended on the fact that, during the experimental tests, only the S_0 waves mode has been recorded. By a numerical point of view, this justifies even more the use of shell elements, which are more efficient in the modelling of the Symmetric modes.

According to Fig. 6, it appears that the damage modeled with reference to the deleting technique and oriented with an angle of 45° provides a better level of accuracy, with reference to the experimental DIs, in terms of damage index prediction.

Moreover, from Fig. 6 it can be noticed that the highest value of damage index is provided by sensor 7. This can be justified by the fact that, according to Fig. 7, the damage is positioned along the pattern actuator 5 (ACT 5) – sensor 7 (PZT 7). As a result, the most difference between the baseline signal and the recorded signal is expected exactly here. The second highest DI has been recorded at sensor 4 (PZT 4). This can be addressed to the largest amount of damage scattered waves; a waves package, in fact, is reflected back from the upper right damage free edge (Fig. 7).

The other DIs, from the highest to the smallest, are recorded at sensor 8 (PZT 8), sensor 9 (PZT 9) and sensor 6 (PZT 6).

The third highest DI is recorded at PZT 8 because it is closer to the damage than PZT 9 and PZT 6. The little difference between the DIs recorded at PZT 6 and PZT 9, which are quite equidistant from the damage, can be addressed to presence of the spar (Fig. 7) which is placed between ACT 5 and PZT 9. DI recorded at PZT 9, in fact, is slightly higher by both numerical and experimental point of views than the DI recorded at PZT 6.

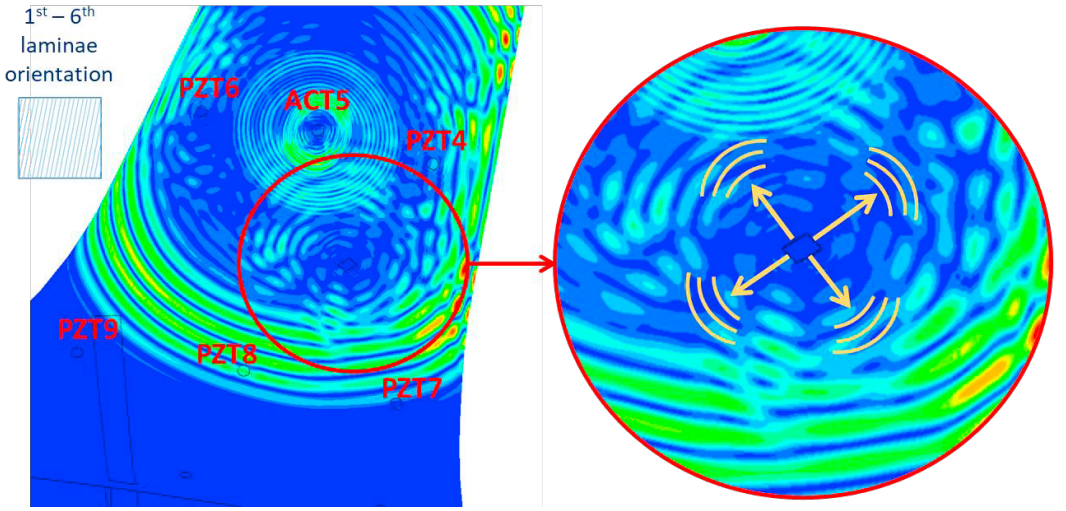

Fig. 7. Damage scattered waves.

Moreover, the fact that the DIs achieved by the simulation involving the 45° oriented damage are in better agreement with experimental results (than the DIs recorded for the 0° oriented damage) can be attributed to the characteristic shape of the LVI damages. LVI damages are usually characterized by a peanut shape with the maximum dimension oriented along the fibers direction. According to Table 2, the first and the last laminae of the winglet skin are unidirectional and oriented with an angle of 0°, whilst the inner ones are of the fabric type (±45°). As a result, even if the square representation is a strong approximation, by rotating it in a way to align one of the diagonals with the first and last laminae fibers orientations, a better approximation can be achieved, because of a more similar shape to the real one.

5. Conclusions

In this paper, two FE damage modelling strategies have been developed to investigate numerically the interaction between Lamb wave propagation and LVI damages. The test article used for such purpose is a GFRP winglet for small aircrafts.

In particular, starting from an established FE model, the numerical investigation has been performed by introducing in this FE model two squared damage types (in two separate analyses) different by each other only for their orientation (0° and 45°). Each damage has been modelled according to two techniques, consisting in degrading the elastic material properties of some finite elements (softening technique) and in deleting the elements (deleting technique), respectively. The signals predicted at the sensors arranged on the damaged winglet have been compared, through the Root Mean Square Deviation Damage Index, with the baseline ones acquired in the pristine configuration.

It was found out that the 45° oriented damage, modelled with reference to the deleting technique, provides the best level of accuracy in terms of damage index prediction. With reference to the 45° orientation, the main reason has been attributed to the fact that LVI damages, distinguishable for their typical peanut shape, find their maximum dimension oriented along the fibers direction. Since the first and the last laminae of the winglet skin are unidirectional and oriented with an angle of 0°, even if the square representation is a strong approximation, by rotating the square in a such way to align one of its diagonals along the fibers direction, a better approximation can be achieved, because of a more similar shape to the typical real one.

References

Caputo, F., De Luca, A., Greco, A., Maietta, S., Bellucci, M., 2018. FE simulation of a SHM system for a large radio–telescope. International Review on Modelling and Simulations 11, 5–14.

Chiu, W.K., Tian, T., Chang, F.K., 2009. The effects of structural variations on the health monitoring of composite structures. Composite Structures 87, 121–140.

Ciminello, M., De Fenza, A., Dimino, I., Pecora, R., 2017. Skin–spar failure detection of a composite winglet using FBG sensors. Archive of Mechanical Engineering 64, 287–300.

De Fenza, A., Petrone, G., Pecora, R., Barile, M., 2017. Post–impact damage detection on a winglet structure realized in composite material. Composite Structures 169, 129–137.

De Fenza, A., Sorrentino, A., Vitiello, P., 2015. Application of Artificial Neural Networks and Probability Ellipse methods for damage detection using Lamb waves. Composite Structures 133, 390–403.

De Luca, A., Caputo, F., Sharif Khodaei, Z., Aliabadi, M.H., 2018. Damage characterization of composite plates under low velocity impact using ultrasonic guided waves. Composites Part B: Engineering 138, 168–180.

De Luca, A., Lamanna, G., Soprano, A., Caputo, F., 2018. Modelling of interactions between Barely Visible Impact Damages and Lamb waves in CFRP laminates. Procedia Structural Integrity 8, 288–296.

De Luca, A., Perfetto, D., Petrone, G., De Fenza, A., Caputo, F., 2018. Guided–waves in a Low Velocity Impacted Composite Winglet. Key Engineering Materials 774, 343–348.

De Luca, A., Sharif–Khodaei, Z., Aliabadi, M.H., Caputo, F., 2016. Numerical Simulation of the Lamb Wave Propagation in Impacted CFRP. Procedia Engineering 167, 109–115.

Frederick, C.L., Worlont, D.C., 1962. Ultrasonic thickness measurements with Lamb waves. Journal of Nondestructive Test 20, 51–55.

Lamb, H., 1917. On waves in an elastic plate. Royal Society of London 93, 114–128.

Lee, B.C., Staszewski, W.J., 2003. Modelling of Lamb waves for damage detection in metallic structures: part I – wave propagation. Smart Materials and Structures 12, 804–814.

Liv, Y.I., Guillamet, G., Costa, J., González, E.V., Marín, L., Mayugo, J.A., 2017. Experimental study into compression after impact strength of laminates with conventional and nonconventional ply orientations. Composite Part B Engineering 126, 133–42.

Lopresto, V., Caprino, G., Leone, C., 2013. A new damage index for the indentation depth evaluation of composites under low velocity impact loads. Polymer Composites 34, 2061–2066.

Mircea, C., Holger, H., 2010. Damage tolerance of composite structures in aircraft industry. Internal Technical Report EADS – Defence and Security.

Reda, M.M. T., Lucero, J., 2005. Damage identification for structural health monitoring using fuzzy pattern recognition. Engineering Structures 27, 1774–1783.

Riccio, A., Damiano, M., Raimondo, A., Di Felice, G., Sellitto, A., 2017. A fast numerical procedure for the simulation of inter–laminar damage growth in stiffened composite panels. Composite Structures 145, 203–216.

Riccio, A., Di Costanzo, C., Di Gennaro, P., Sellitto, A., Raimondo, A., 2017. Intra–laminar progressive failure analysis of composite laminates with a large notch damage. Engineering Failure Analysis 73, 97–112.

Riccio, A., Sellitto, A., Saputo, S., Russo, A., Zarrelli, M., Lopresto, V., 2017. Modelling the damage evolution in notched omega stiffened composite panels under compression. Composites Part B: Engineering 126, 60–71.

Rose, J.L., 2001. A vision of ultrasonic guided wave inspection potential. 7th ASME NDT Topical Conference, San Antonio, Texas USA, 20, 1–5.

Russo, P., Langella, A., Papa, I., Simeoli, G., Lopresto, V., 2017. Thermoplastic polyurethane/glass fabric composite laminates: Low velocity impact behavior under extreme temperature conditions. Composite Structures 166, 146–152.

Sepe, R., De Luca, A., Lamanna, G., Caputo, F., 2016. Numerical and experimental investigation of residual strength of a LVI damaged CFRP omega stiffened panel with a cut–out. Composites Part B: Engineering 102, 38–56.

Sharif–Khodaei, Z., Aliabadi, M.H., 2014. Assessment of delay–and–sum algorithms for damage detection in aluminium and composite plates. Smart Materials and Structures 23, paper #075007.

Sorrentino, A., De Fenza, A., 2017. Damage detection in complex composite material structures by using elliptical triangulation method. 11th International Workshop on Structural Health Monitoring, Stanford, California, USA.

Sorrentino, A., De Fenza, A., 2017. Improved elliptical triangulation method for damage detection in composite material structures. Journal of Mechanical Engineering Science – Special Issue on SHM 231, 3011–3023.

Sorrentino, A., De Fenza, A., Romano, F., Mercurio, U., 2018. Experimental application of Lamb wave based SHM system at complex composite material structures. 9th Workshop on Structural Health Monitoring, Manchester, UK.

Su, Z., Ye, L., 2009. Identification of Damage Using Lamb Waves. In: Pfeiffer, F., Wriggers, P. (Ed.). Lecture Notes in Applied and Computational Mechanics 48.

Worden, K., Dulieu–Barton, J.M., 2004. An Overview of Intelligent Fault Detection in Systems and Structures. Structural Health Monitoring 3, 85–98.

Worlont, D.C., 1961. Experimental confirmation of Lamb waves at megacycle frequencies. Journal of Applied Physics 32, 967–971.